Bioorganic & Medicinal Chemistry Letters 24 (2014) 5769–5776

Contents lists available at ScienceDirect

Bioorganic & Medicinal Chemistry Letters

journal homepage: www.elsevier.com/locate/bmcl

# A reversed sulfonamide series of selective RORc inverse agonists

Monique B. van Niel [a,*], Benjamin P. Fauber [b], Matthew Cartwright [a], Simon Gaines [a], Jonathan C. Killen [a], Olivier René [b], Stuart I. Ward [a], Gladys de Leon Boenig [b], Yuzhong Deng [b], Céline Eidenschenk [b], Christine Everett [b], Emanuela Gancia [a], Arunima Ganguli [a], Alberto Gobbi [b], Julie Hawkins [a], Adam R. Johnson [b], James R. Kiefer [b], Hank La [b], Peter Lockey [a], Maxine Norman [a], Wenjun Ouyang [b], Ann Qin [b], Nicole Wakes [a], Bohdan Waszkowycz [a], Harvey Wong [b]

[a] Argenta, Early Discovery, Charles River, 7-9 Spire Green Centre, Flex Meadow, Harlow, Essex CM19 5TR, United Kingdom
[b] Genentech, Inc., 1 DNA Way, South San Francisco, CA 94080, USA

ARTICLE INFO

*Article history:*
Received 5 September 2014
Revised 9 October 2014
Accepted 14 October 2014
Available online 25 October 2014

*Keywords:*
RORc
RORγ
RORγt
IL-17
Inflammation
X-ray structure

ABSTRACT

The identification of a new series of RORc inverse agonists is described. Comprehensive structure-activity relationship studies of this reversed sulfonamide series identified potent RORc inverse agonists in biochemical and cellular assays which were also selective against a panel of nuclear receptors. Our work has contributed a compound that may serve as a useful in vitro tool to delineate the complex biological pathways involved in signalling through RORc. An X-ray co-crystal structure of an analogue with RORc has also provided useful insights into the binding interactions of the new series.



A large family of 48 nuclear receptors (NRs) has been characterised in humans and natural ligands are known for approximately half of the members.[1] The architecture of NRs forms five common domains including an amino-terminal activation domain (AF-1), a second activation domain (AF-2), a DNA binding domain (DBD), a hinge region, and a hydrophobic ligand binding domain (LBD) located at the C-terminus.[2] Binding of ligands in the LBD causes a conformational change which increases or decreases the recruitment of large proteins, a key process that is required to influence downstream gene regulation.[3] Ligands are classified according to their role in increasing or decreasing the protein recruitment. The term inverse agonist is used when ligands induce conformational changes in the protein which reduce the recruitment of co-activator proteins and leads to the silencing of target gene expression.[4] Conversely, the term agonist is used for ligands which increase co-activator recruitment and results in enhanced gene expression. There is a continuum between these two extreme states. Ligands can also be termed antagonists if they reverse the activity of an agonist-induced system or silent ligands if they bind but induce no functional effect on the system. In addition, partial agonists increase transcription but do so to a lesser extent than full agonists, and partial inverse agonists elicit reduced efficacy relative to the response of a full inverse agonist.

Retinoic acid receptor-related orphan receptors (RORs) are new members of the NR family which show constitutive activity in the absence of ligands.[3] Isoforms of ROR (human isoforms RORa, b and c are also known as RORα, β and γ) are involved in a variety of physiological processes and have distinct patterns of tissue distribution.[5] Murine RORγ exists as two isoforms, termed RORγ and RORγt, which have played a critical role in developing an understanding of the pathway and functioning of this NR. Tissue distribution of the RORγ isoforms show high levels of expression in thymus and lower levels in immune tissue, liver, skeletal muscle, adipose tissue and kidney. Of particular interest is the involvement of RORγt in the differentiation and function of interleukin (IL)-17 producing helper T ($T_H17$) cells. Animal studies suggest that the modulation of IL-17 levels in autoimmune diseases including multiple sclerosis, psoriasis, inflammatory bowel disease and rheumatoid arthritis (RA) may be beneficial in terms of disease progression.[6]

Although RORc is classed as an orphan receptor since no natural ligand has been unambiguously identified,[7] some structurally complex natural products derived from cholesterol, sterol ligands,

* Corresponding author. Tel.: +44 1279 645645.
*E-mail address:* Bodil.vanniel@crl.com (M.B. van Niel).

http://dx.doi.org/10.1016/j.bmcl.2014.10.037
0960-894X/

cholanoic acid and digoxin are documented to bind with high affinities.[8] The putative endogenous ligands 20α-, 22(*R*)- and 25-hydroxycholesterol (**1**, **2**, **3**, Fig. 1) have high affinity for RORc ($EC_{50}$ = 20–40 nM)[9] and have crystallographically characterised binding modes similar to known agonists of other NRs.[10] A co-crystal structure with digoxin (**4**, Fig. 1) demonstrated that the ligand-induced disruption of the ordered structure of helices 11, 11′ and 12 resulted in an inverse agonist profile ($K_d$ = 109 nM).[11–13] These potent, lipophilic ligands form predominantly van der Waals contacts with the largely hydrophobic ligand-binding pocket of RORc. This information gave an early indication of the future challenges that would be faced in identifying small molecule ligands for RORc with appropriate physicochemical properties commensurate with drug development. Whilst **1**–**4** have served as important tool compounds, these molecules were not viewed as optimal starting points for further optimisation due to their high molecular weight, lipophilicity and complex synthesis required for scaffold modifications.

Since the first disclosure of RORc in the 1990s,[14] efforts to identify small molecule modulators to characterise the role of RORc in inflammatory processes using in vivo models have gained momentum.[15] The experimental autoimmune encephalomyelitis model of multiple sclerosis,[12,13,16,17] mouse psoriasis model,[18,19] and mouse collagen-induced arthritis models[20] involve $T_H17$ cells and have been used to probe disease progression using small molecule RORc modulators. Although clinical trials using human monoclonal antibodies which target IL-17 have shown efficacy in RA, psoriasis and uveitis,[21] the validation of the RORc pathway with small molecules in clinical trials has only recently started,[22] some 20 years after RORc was discovered. The continued progression and evaluation of selective, orally bioavailable small molecules in clinical trials will help to define the role of RORc as a target to modulate IL-17 in human diseases and offers potential to identify new treatments for debilitating autoimmune diseases in man.

Following the disclosure of the first small molecule RORa/c inverse agonist T0901317 (**5**, Fig. 2),[23] it has been interesting to observe evolving structure-activity relationships (SAR) which have successfully identified less promiscuous, but low affinity inverse agonists including SR1001 (**6**, Fig. 2).[17,24] A diverse range of small molecule chemotypes have been disclosed as the interest in RORc has intensified. A comprehensive review covering the literature up to 2014 discusses RORc as a target and has usefully collated all available information on small molecule RORc ligands from patents and publications.[25] The considerable structural diversity of reported ligands suggests that RORc functional response requires few specific ligand–protein interactions. There is a high prevalence of functional groups such as amides, sulfonamides and carboxylic acids whilst multiple aryl rings are commonly encountered in the ligands reported to date. These structurally diverse ligands, with lower molecular weight but generally high lipophilicities, continue to be useful tools in delineating the complex biological pathways involved in signalling through RORc.

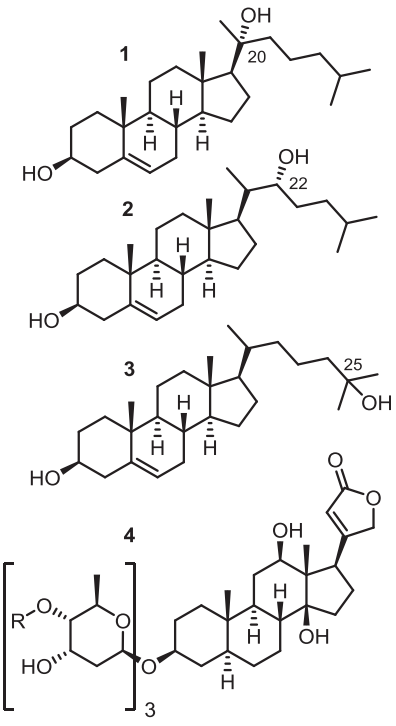


**Figure 1.** Natural product RORc ligands.

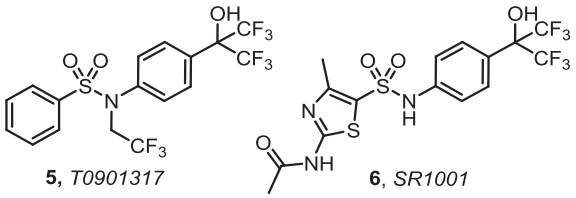


**Figure 2.** Examples of small molecule RORc inhibitors.

The Genentech RORc program targeted the identification of selective, small molecule inverse agonists which could be progressed in vivo, and a new series of tertiary sulfonamide compounds derived from a NR compound subset of the Genentech/Roche corporate compound collection has recently been reported.[26] Compounds **7**–**9** (Table 1) containing a bi-aryl core and H-bond donor/acceptor functional groups, were demonstrated to be potent RORc inverse agonists with appreciable selectivity over ROR isoforms and other NRs. A co-crystal structure of **7** in the RORc binding pocket revealed that disruption of protein H-bonds seen in agonist structures resulted in the inverse agonist character of the series (vide infra). The overall profile of these compounds was sufficiently interesting to expand SAR exploration and a further publication has described the outcomes of this work.[27]

Herein we report our findings aimed at identifying a second series by transposing the sulfonamide group to generate a parallel series with the linker atoms reversed.[28] Our screening cascade also used the previously reported biochemical assays.[29] A radiometric binding assay monitored the displacement of [$^3$H]25-hydroxycholesterol from the RORc-LBD. A separate time-resolved fluorescence biochemical assay monitored the ability of the human RORc-LBD to bind to a co-activator peptide derived from steroid receptor co-activator-1 (SRC1).[29] In this assay, a compound that disrupted the recruitment of the SRC1 co-activator peptide to RORc was termed a RORc inverse agonist.

Early SAR showed that transposing the sulfonamide linker of **9** to give tertiary phenethylamine analogue **10** (Table 1) retained an equivalent potency in the competitive binding assay. However, **10** showed a maximum inhibition of only 40% in the SRC1 co-activator peptide recruitment assay which contrasted with the high potency and strong RORc inverse agonist efficacy seen with **9** ($EC_{50}$ = 21 nM, −94% efficacy). The methylene spaced analogue (**11**) which maintained an equivalent four linking atoms between the aryl rings maintained a potent RORc binding ($IC_{50}$ = 66 nM) and inverse agonist profile ($EC_{50}$ = 0.32 μM, −79% efficacy) compared to **10**. It was anticipated that synthesis of further analogues based on **10** would be more straightforward compared to **11** and we therefore focused on this option during subsequent SAR campaigns. The ligand-lipophilicity efficiencies (LLE = $pIC_{50}$-*c*Log*P*)[30] for **10** and

**Table 1**
Structures of lead sulfonamide **7** and new reversed sulfonamide analogues

| Compd | Structure | RORc $IC_{50}$[a] (μM) | RORc LLE[b] | RORc SRC1 $EC_{50}$[c] (μM) [%eff.] |
|---|---|---|---|---|
| **7** | 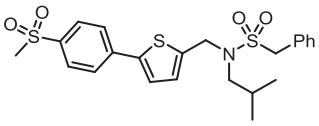 | 0.13 | 2.6 | 0.46 [−72%] |
| **8** | 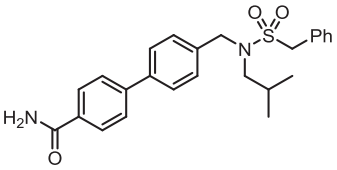 | 0.033 | 2.9 | 0.040 [−90%] |
| **9** | 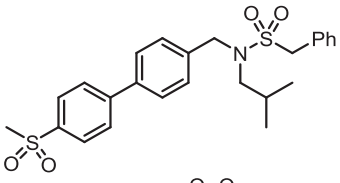 | 0.032 | 3.0 | 0.021 [−94%] |
| **10** | 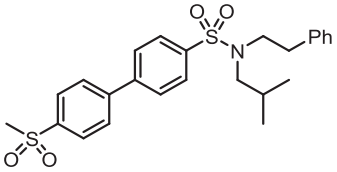 | 0.037 | 2.2 | 1.0 [−40%] |
| **11** | 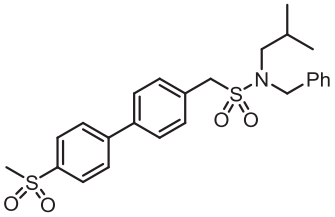 | 0.066 | 2.7 | 0.32 [−79%] |
| **12** | 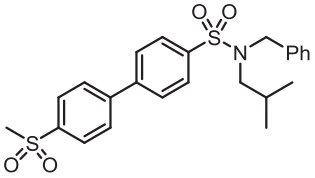 | 0.16 | 1.9 | >20 [−20%] |

See Ref. 29 Supplementary data for experimental details of all assays. All assay results are reported as the geometric mean of at least two separate runs.
[a] Biochemical inhibition of the RORc LBD and [$^3$H]25-hydroxycholesterol interaction.
[b] Lipophilic ligand efficiency (LLE) was calculated using the RORc biochemical $IC_{50}$ value and calculated log*P* (*c*Log*P*).[26]
[c] Inhibition of RORc LBD recruitment of the SRC1 co-activator peptide; negative percent efficacy '%eff.' denotes inverse agonism relative to the basal activity of apo-RORc LBD in this assay format. The maximum concentration tested was 10 μM in this assay except for compound **12** which was tested up to 20 μM.

**11** were lower when compared to **9**. Whilst LLE was an important consideration, this metric is reported using data from the biochemical binding assay and we also had to consider the wider implications of the data from the SRC1 co-activator peptide recruitment assay on the overall profile when deciding which leads should be further investigated. A truncated tertiary benzylamine analogue **12** had reasonable binding potency ($IC_{50}$ = 160 nM), but it was nearly a silent ligand in the SRC1 co-activator peptide recruitment assay, showing a maximum inhibition of only 20% at 20 μM, the highest test concentration. This co-activator recruitment result suggested that the relative location of the sulfonamide linker could modulate inverse agonism. Additional SAR extensively explored substitution on the aryl rings of the phenethylamine (**10**) and benzylamine (**12**) reversed sulfonamides in an attempt to disrupt the intact *C*-terminus, as had been observed in the co-crystal of **7**.[26] Although strong binding affinity in the human RORc-LBD could be achieved by other analogues (data not shown), they were still only partial inverse agonists or silent ligands in the SRC1 co-activator peptide recruitment assay. These data continued to highlight areas that would require significant improvement if the reversed sulfonamides were to become a viable alternative series.

From this preliminary SAR, it was clear that optimisation of the profile in the SRC1 co-activator peptide recruitment assay together with improvements of physicochemical properties were required to advance the series. To progress the new series at a fast pace we split exploration into three areas. Interactions on the left-hand side (LHS) were explored using a small selection of polar groups to conserve potential H-bonding interactions with the RORc protein. In addition, we noted that changes to the bi-aryl core which occupied the central portion of the binding site should in principle be tolerated due to the available space and the flexibility of the aliphatic side-chains lining the pocket. Finally, the right-hand side (RHS) of the ligand was the focus of modifications aimed at increasing the level of the inverse agonism. Due to the large number of aromatic residues on the RHS of the pocket and the potential for π–π interactions, we decided to maintain an aromatic ring in that region and concentrated our efforts on modifying the linker length and investigating substitution around the ring.

The lipophilicity of reversed sulfonamide leads **10**–**12** was high (*c*Log*P*[26] 4.5–5.2), and we designed compounds such that parameters were in a range considered to be desirable property space for oral drugs (*c*Log*P* <4 was preferred).[31–33] The aqueous solubility of the early reversed sulfonamide leads **10**–**12** was low (<1 μM at pH 7.4) and there is mounting literature evidence that multiple aryl rings can be detrimental to this property.[34–36] Encouraged by the reported SAR in the parent sulfonamide series,[27] replacing the aryl ring of **12** located in the hydrophilic region of the binding site with non-aromatic heterocycles was investigated (Table 2). Morpholine (**13**) and 4-hydroxypiperidine (**14**) analogues were substantially less potent in the binding assay, indicating that these H-bond acceptor/donor groups were not optimal at the terminal region of the molecules. The basic *N*-methylpiperazine (**15**) showed a further significant reduction in binding potency. Modest affinity for RORc could be regained by introduction of *N*-acetyl- (**16**), *N*-sulfamoyl– (**17**) and *N*-methanesulfonyl– (**18**) substituents on the piperazine to reduce basicity and these analogues had reduced lipophilicity (*c*Log*P* 2.6–3.9). We noted that **17** and **18** had improved LLE values (4.2 and 3.1, respectively), but disappointingly all *N*-linked heterocyclic ring analogues (**13**–**18**) had less than 50% inhibition in the SRC1 peptide co-activator recruitment assay at the highest test concentration. The homologue (**19**) had marked potency improvements in RORc binding ($IC_{50}$ = 51 nM) when compared to **18** ($IC_{50}$ = 0.37 μM).

Subsequent SAR was generated using the *N*-methanesulfonylpiperazine as a ligand-anchor since this *N*-linked heterocyclic ring was straightforward to introduce, chemically benign during synthesis and the overall lipophilicity of **18** was reasonable (*c*Log*P* = 3.3). We next investigated modifications of the central phenyl ring. Fluorine *ortho* or *meta* to the sulfonamide linker of **18** resulted in a large improvement in binding potencies when combined with the tertiary benzylamine (**20**, $IC_{50}$ = 93 nM; **21**, $IC_{50}$ = 51 nM). The combination of fluorine substitution with a longer tertiary phenethylamine resulted in equipotent binding affinities for **22** and **23** ($IC_{50}$ = 41 nM). However, there was again a clear preference for higher potencies in the SRC1 co-activator peptide recruitment assay for the longer side chains of **22** and **23** as had previously been observed when comparing **10** with **12**. Identification of **22** demonstrated for the first time that potent binding and a high affinity and high efficacy inverse agonist profile could be achieved in this reversed sulfonamide series. We also replaced the central aryl ring with pyridine isomers (**24**–**27**) as a way to moderate the overall lipophilicity of the chemical series. Although pyridines **24**–**27** successfully lowered the *c*Log*P* by 0.5–0.8 units compared to **18** and **19**, these heterocycles were also less potent in both biochemical assays. A range of other six-membered ring heterocycles including pyrimidine, pyridazine and pyrazine showed large reductions in binding potencies (data not shown) and these observations are in line with our previously reported data in the parent sulfonamide series.[27]

We next targeted aryl ring substitution of the tertiary benzylamine (**18**) and phenethylamine (**19**) since these bind in the region of the RORc-LBD likely to cause disordering of the H-bond between H479 and Y502.[11] A scan of chloro substitution showed a modest preference for *ortho* substitution (**28**) in the RORc biochemical binding assay. Whilst *meta* (**29**) and *para*-chloro benzylamines (**30**) were equipotent in the binding assay, slightly stronger inverse agonist potency was obtained for **30**. A large body of follow-up work showed *ortho*-trifluoromethylbenzyl amine (**31**) achieved high binding potency and considerably higher efficacy than had been observed with the corresponding *ortho*-chloro benzylamine analogue (**28**). Obtrusion into this region of the binding site by **31** presumably resulted in disruption of helices 11′–12, which

**Table 2**
Piperidine and piperazine analogues

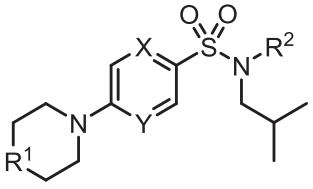


| Compd | $R^1$-group | X | Y | $R^2$-group | RORc $IC_{50}$[a] (μM) | RORc LLE[b] | RORc SRC1 $EC_{50}$[c] (μM) [%eff.] | *c*Log*P*[b] |
|---|---|---|---|---|---|---|---|---|
| **13** | O | C—H | C—H | $PhCH_2$– | 0.51 | 2.1 | >6.7 [−12%] | 4.2 |
| **14** | CH—OH | C—H | C—H | $PhCH_2$– | 0.44 | 1.8 | >20 [−29%] | 4.6 |
| **15** | N—$CH_3$ | C—H | C—H | $PhCH_2$– | 5.6 | 0.85 | >20 [−16%] | 3.8 |
| **16** | N—$COCH_3$ | C—H | C—H | $PhCH_2$– | 0.42 | 2.5 | >10 [−29%] | 3.9 |
| **17** | N—$SO_2N(CH_3)_2$ | C—H | C—H | $PhCH_2$– | 0.17 | 4.2 | >10 [−3%] | 2.6 |
| **18** | N—$SO_2CH_3$ | C—H | C—H | $PhCH_2$– | 0.37 | 3.1 | 0.53 [−29%] | 3.3 |
| **19** | N—$SO_2CH_3$ | C—H | C—H | $PhCH_2CH_2$– | 0.051 | 3.6 | 0.34 [−55%] | 3.7 |
| **20** | N—$SO_2CH_3$ | C—F | C—H | $PhCH_2$– | 0.093 | 3.4 | >10 [−42%] | 3.6 |
| **21** | N—$SO_2CH_3$ | C—H | C—F | $PhCH_2$– | 0.051 | 3.9 | >10 [−20%] | 3.4 |
| **22** | N—$SO_2CH_3$ | C—F | C—H | $PhCH_2CH_2$– | 0.042 | 3.5 | 0.05 [−85%] | 3.9 |
| **23** | N—$SO_2CH_3$ | C—H | C—F | $PhCH_2CH_2$– | 0.041 | 3.6 | 0.15 [−48%] | 3.8 |
| **24** | N—$SO_2CH_3$ | N | C—H | $PhCH_2$– | 0.43 | 3.6 | >10 [−36%] | 2.8 |
| **25** | N—$SO_2CH_3$ | N | C—H | $PhCH_2CH_2$– | 0.19 | 3.5 | 4.5 [−55%] | 3.2 |
| **26** | N—$SO_2CH_3$ | C—H | N | $PhCH_2$– | 0.34 | 3.9 | >10 [−24%] | 2.6 |
| **27** | N—$SO_2CH_3$ | C—H | N | $PhCH_2CH_2$– | 0.16 | 3.9 | 0.34 [−38%] | 2.9 |
| **28** | N—$SO_2CH_3$ | C—H | C—H | (2-Cl) $PhCH_2$– | 0.021 | 3.8 | >10 [−35%] | 3.9 |
| **29** | N—$SO_2CH_3$ | C—H | C—H | (3-Cl) $PhCH_2$– | 0.070 | 3.1 | >10 [−13%] | 4.1 |
| **30** | N—$SO_2CH_3$ | C—H | C—H | (4-Cl) $PhCH_2$– | 0.061 | 3.1 | 1.3 [−72%] | 4.1 |
| **31** | N—$SO_2CH_3$ | C—H | C—H | (2-$CF_3$) $PhCH_2$– | 0.034 | 3.3 | 0.10 [−63%] | 4.2 |
| **32** | N—$COCH_3$ | C—H | C—H | (2-$CF_3$) $PhCH_2$– | 0.0092 | 3.2 | 0.085 [−81%] | 4.8 |

See Ref. 29 Supplementary data for experimental details of all assays. All assay results are reported as the geometric mean of at least two separate runs.

[a] Biochemical inhibition of the RORc LBD and [$^3$H]25-hydroxycholesterol interaction.

[b] Lipophilic ligand efficiency (LLE) was calculated using the RORc biochemical $IC_{50}$ value and calculated log*P* (*c*Log*P*) [26].

[c] Inhibition of RORc LBD recruitment of the SRC1 co-activator peptide; negative percent efficacy '%eff.' denotes inverse agonism relative to the basal activity of apo-RORc LBD in this assay format. The maximum concentration tested was 10 μM in this assay except for compound **19** which was tested up to 200 μM.

contrasts with substituents like *para*-chloro benzylamine (**30**) that may adopt an appropriate vector for the *para* substituent to cause a similar disruption. At this stage of our SAR, we re-evaluated the *N*-acetyl piperazine (**32**) which confirmed our earlier observations with **16** and **17** that a number of H-bond acceptors are able to maintain equivalent profiles in the biochemical assays.

The identification of reversed aryl sulfonamides with greater inverse agonism efficacy encouraged us to investigate the introduction of linker atoms at alternative locations in the scaffold to act as a spacer between the ligand–anchoring interactions of the *N*-methanesulfonyl piperazine group and the LHS terminal aryl ring (Table 3). This strategy could be considered complementary to our initial efforts to use phenethylamine compared to benzylamine. We modified the *N*-methanesulfonyl piperazine (**31**) to the corresponding 4-amino-*N*-methanesulfonyl piperidine (**33**). This strategy also relaxed some conformational rigidity which may have harmonised the fit of reversed sulfonamides in the binding site. Identification of **33** ($IC_{50}$ = 6 nM; $EC_{50}$ 12 nM, −91% efficacy) resulted in the first example from the new reversed sulfonamide series with single digit nanomolar binding affinity while also displaying potent and high efficacy RORc inverse agonism. The homologue (**34**, $IC_{50}$ = 33 nM; $EC_{50}$ = 28 nM, −91% efficacy) gave a similar overall profile in the biochemical assays as the corresponding piperazine (**31**, $IC_{50}$ = 34 nM; $EC_{50}$ = 100 nM, −63% efficacy). Opportunities to introduce polar functionality had been limited in the reversed sulfonamide series and additional linker groups were investigated starting with the ether (**35**) which had a six-fold improvement in binding potency when compared to **31**. The synthetically versatile carbonyl linker (**36**) was also prepared and reduced to the racemic secondary alcohol (**37**) and eliminated to the alkene (**38**) to give analogues which retained a high binding potency and similar overall profile to **35**. This suggested that this region of the scaffold could usefully be exploited to introduce polar functionality which may be able to interact with polar residues in the RORc binding pocket or interact with the water architecture in the RORc-LBD.

The overall lipophilicity of these new analogues containing a spacer group was still high (*c*Log*P* >4) and our aim was to re-optimise substitution of the terminal aryl ring to manipulate the overall physicochemical properties of the series. The ether linker was conserved during this work since it was facile to introduce 4-hydroxy-*N*-methanesulfonyl piperidine as the last step through simple displacement of a *para*-fluoro substituent on the appropriate benzene sulfonamide fragment.[28] A scan of *ortho*-(**39**), *meta*-(**40**) and *para*-fluorine (**41**) substituents on the terminal aryl ring confirmed that the *meta*- and *para*- substitution were most potent. A nitrile (**42–44**) substitution scan showed that analogues which retained high binding potencies and strong inverse agonist profiles with reduced lipophilicity (*c*Log*P* 3.8) could be identified through modifications of the terminal aryl ring.

Replacement of the terminal aryl ring with polar heterocycles was also investigated as part of our ongoing strategy to reduce lipophilicity of the ether linked series. However, pyridines **45** and **46** gave disappointing potency in both biochemical assays and this region of the RORc-LBD appears to be unable to tolerate polar functionality. We also replaced the *N*-isobutyl group and investigated a small set of alternative alkyl groups. Although reasonable binding potency could be maintained, disappointingly, alternative substituents including *N*-*tert*-butyl, *N*-methylcyclobutyl, *N*-cyclobutyl, *N*-trifluoroethyl and *N*-isopentyl amines all had low inverse agonist potency (data not shown) and we did not further investigate other substituents with more polar overall properties. The data confirmed that there was an optimal steric contribution of the *N*-isobutyl group in maintaining the overall biochemical profile of the reversed sulfonamide series. Our observations contrast with the parent sulfonamide series where a selection of small aliphatic or halogenated groups could improve RORc inverse agonist potency, reduce lipophilicity and increase aqueous solubility.[27]

Finally, we investigated a combination of all beneficial changes and a number of analogues were prepared including the 4-amino or 4-hydroxy *N*-methanesulfonyl piperidine scaffold and a central

**Table 3**
Piperidine analogues

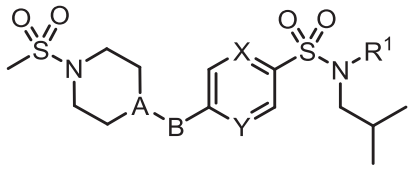


| Compd | A-B | X | Y | $R^1$-group | RORc $IC_{50}$[a] (μM) | RORc LLE[b] | RORc SRC1 $EC_{50}$[c] (μM) [%eff.] | *c*Log*P*[b] |
|---|---|---|---|---|---|---|---|---|
| **33** | CH—NH | C—H | C—H | (2-$CF_3$) $PhCH_2$– | 0.006 | 3.3 | 0.012 [−91%] | 4.9 |
| **34** | CH—NH | C—H | C—H | (2-$CF_3$) Ph– | 0.033 | 2.5 | 0.028 [−68%] | 5.0 |
| **35** | CH—O | C—H | C—H | (2-$CF_3$) $PhCH_2$– | 0.006 | 3.4 | 0.022 [−90%] | 4.8 |
| **36** | CH—C(O) | C—H | C—H | (2-$CF_3$) $PhCH_2$– | 0.007 | 3.6 | 0.056 [−82%] | 4.5 |
| **37** | CH—CH(OH) | C—H | C—H | (2-$CF_3$) $PhCH_2$– | 0.011 | 3.9 | 0.022 [−88%] | 4.0 |
| **38** | C=CH | C—H | C—H | (2-$CF_3$) $PhCH_2$– | 0.014 | 2.2 | 0.075 [−84%] | 5.6 |
| **39** | CH—O | C—H | C—H | (2-F) Ph– | 0.056 | 3.1 | 0.06 [−79%] | 4.1 |
| **40** | CH—O | C—H | C—H | (3-F) Ph– | 0.008 | 3.8 | 0.021 [−91%] | 4.3 |
| **41** | CH—O | C—H | C—H | (4-F) Ph– | 0.016 | 3.5 | 0.022 [−97%] | 4.3 |
| **42** | CH—O | C—H | C—H | (2-CN) Ph– | 0.021 | 3.9 | 0.068 [−52%] | 3.8 |
| **43** | CH—O | C—H | C—H | (3-CN) Ph– | 0.014 | 4.0 | 0.059 [−85%] | 3.8 |
| **44** | CH—O | C—H | C—H | (4-CN) Ph– | 0.015 | 4.0 | 0.027 [−96%] | 3.8 |
| **45** | CH—O | C—H | C—H | 2-Pyridyl– | 0.17 | 3.6 | 0.24 [−63%] | 3.2 |
| **46** | CH—O | C—H | C—H | 3-Pyridyl– | 0.18 | 3.8 | 0.49 [−75%] | 3.0 |
| **47** | CH—O | N | C—H | (2-$CF_3$) $PhCH_2$– | 0.012 | 3.6 | 0.015 [−89%] | 4.3 |
| **48** | CH—NH | C—H | N | (4-F) $PhCH_2$– | 0.18 | 3.2 | 0.52 [−64%] | 3.6 |

See Ref. 29 Supplementary data for experimental details of all assays. All assay results are reported as the geometric mean of at least two separate runs.

[a] Biochemical inhibition of the RORc LBD and [$^3$H]25-hydroxycholesterol interaction.

[b] Lipophilic ligand efficiency (LLE) was calculated using the RORc biochemical $IC_{50}$ value and calculated log*P* (*c*Log*P*).[26]

[c] Inhibition of RORc LBD recruitment of the SRC1 co-activator peptide; negative percent efficacy '%eff.' denotes inverse agonism relative to the basal activity of apo-RORc LBD in this assay format. The maximum concentration tested was 10 μM in this assay.

pyridine ring in combination with a range of tertiary sulfonamide substituents. One highlight from this work was that introduction of pyridine into the scaffold of **35** to give **47** resulted in a similar overall profile with a reduction of lipophilicity (*c*Log*P* 4.8 to 4.3). Although only low inverse agonism (−64% efficacy) was obtained with a second pyridine analogue (**48**), a further highlight was a 1.7 Å resolution co-crystal structure of this compound at the RORc binding site (Fig. 3).[37] In this structure, the compound extended nearly the entire length of the binding site from the hydrophobic region near helices 11 and 12 to the hydrophilic opposite end. Van der Waals interactions dominated the interaction between RORc and **48** (Fig. S1), but two hydrogen bonds linked the terminal methyl sulfone to the protein (side chain of R367 and main chain of L287). Several water molecules bordered the compound and filled the breadth of the pocket; however, only a single solvent H-bond was observed, linking the pyridyl nitrogen to a portion of this solvent shell. A second water molecule resided 3.1 Å from the central amine but was out of geometric alignment for the interaction to be significant. Interestingly, the amino piperidine adopted an atypical axial geometry[37] (*A*-value = 1.9 kcal/mol) that caused the compound to follow a serpentine path through the binding site, in stark contrast to most other ligands which adopted an 'L' shape.[25] This conformation was definitively supported by the unbiased electron density (Fig. S2).

At the hydrophobic end of the pocket, the *para*-fluoro-phenyl substituent packed within the lipophilic pocket defined by residues C320, L324, W317, I400, and L396. In the RORc crystal structure, **48** did not perturb the hydrogen bond between H479 and Y502 that anchored helix 12 in an agonist conformation. As a result, this crystal was obtained in the presence of co-activator peptide and represented the 'agonist mode' of the protein conformation, consistent with **48** only showing low efficacy ($EC_{50}$ = 0.52 μM, −64% efficacy) to displace the SRC1 peptide in the co-activator recruitment assay. In contrast, the previously reported structure of **7** from the sulfonamide series bound to RORc (PDB 4QM0) had its terminal phenyl substituent positioned such that it would clash with the agonist mode position of W317, preventing the protein from adopting an agonist conformation of the *C*-terminus of the protein. Although compounds **7** and **48** differed by a single heavy atom in length (including the fluorine in **48**), the paths that the two molecules traversed through the binding site diverged and gave rise to a 1.0 Å offset of sulfur atom positions at the hydrophilic end and a 2.7 Å separation of equivalent positions of the phenyl rings at the lipophilic end of the pocket. In addition, the phenyl rings were oriented offset from each other by approximately 23°, as measured from the most apical position. The reversing of the sulfonamide connectivity and removal of one bridging atom in the linker moving from **7** to **48** significantly altered the positioning of the hydrophobic region of the ligands (Fig. S3), explaining the separation in SAR for the two series.[37] Additional X-ray data for analogues which had improved binding potency and inverse agonist efficacy may offer insight into the interactions which successfully disrupt the *C*-terminus. Whilst this was highly desirable and actively pursued, successful co-crystallisation of additional reversed sulfonamide examples has remained elusive.

Next we profiled several of the more potent compounds into HEK293 cell based assays using Gal4-NR constructs to assess selectivity profiles in the three isoforms of ROR (Table 4). In addition, we also investigated the selectivity profiles for these analogues against farnesoid X receptor (FXR), pregnane X receptor (PXR) and liver X receptor alpha (LXRα) and liver X receptor beta (LXRβ) using the same cell assay system.[29] The parent sulfonamide **9** was a weak inhibitor in the RORc Gal4 cellular assay ($EC_{50}$ = 453 nM) and was only ~ five-fold selective over the RORa and RORb isoforms and at least 21-fold selective over FXR, LXRα, LXRβ and PXR. Pleasingly, progression of **33**, **34**, **41**, **44** and **47** through the Gal4 cellular assays clearly highlighted that excellent RORc potency and selectivity over the RORa and RORb isoforms could be obtained with these reversed sulfonamides. Weak activity at FXR, LXRα, LXRβ and PXR was observed, which together with the improved RORc

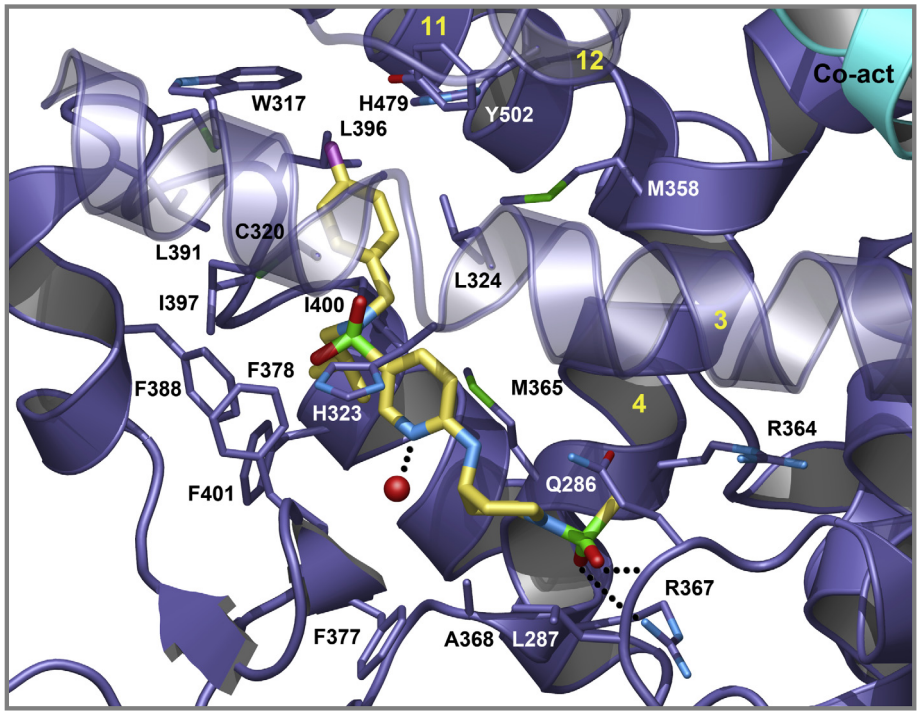


**Figure 3.** Co-crystal structure of **48** (gold) in complex with RORc in an agonist conformation (violet) and co-activator peptide (cyan).[38] Residues within van der Waals' contact of the inhibitor are shown (except where removed for clarity). Amino acids are labelled with single letter code, and key protein helices are annotated numerically in yellow font.

**Table 4**
RORc potency and selectivity profiles in Gal4 human transcription and human IL-17 and cytokine biosynthesis assays

| Compd | RORc Cell $EC_{50}$[a] (μM) | RORa Cell $EC_{50}$[a] (μM) | RORb Cell $EC_{50}$[a] (μM) | FXR Cell $EC_{50}$[a] (μM) | LXRα Cell $EC_{50}$[a] (μM) | LXRβ Cell $EC_{50}$[a] (μM) | PXR Cell $EC_{50}$[a] (μM) | IL-17A hPBMC $EC_{50}$[b] (μM) | IL-17A hPBMC[b] %max. | IFNγ $EC_{50}$ (μM) | CTG $EC_{50}$ (μM) |
|---|---|---|---|---|---|---|---|---|---|---|---|
| **9** | 0.453 | 2.4 | 2.5 | >10 | >10 | >10 | >10 | n.d. | n.d. | n.d. | n.d. |
| **33** | 0.006 | 4.4 | 3.8 | >10 | >10 | >10 | >10 | 0.27 | 73 | >20 | >20 |
| **34** | 0.007 | >10 | >10 | >10 | >10 | >10 | >10 | 0.044 | 67 | >20 | >20 |
| **41** | 0.019 | >10 | >10 | >10 | >10 | >10 | >10 | 0.42 | 67 | >20 | >20 |
| **44** | 0.032 | 8.8 | >8 | >10 | >10 | >10 | >10 | 0.76 | 77 | >20 | >20 |
| **47** | 0.039 | >7.1 | >3.1 | >10 | >10 | >10 | >10 | 0.33 | 68 | >18 | >20 |

See Ref. 29 Supplementary data for experimental details of all assays. All assay results are reported as the geometric mean of at least two separate runs.
[a] All assays were conducted in HEK293 cells using Gal4-NR constructs. All ROR and NR assays monitored the suppression of their respective basal transcriptional activities, an outcome consistent with inverse agonist activity of ligands with these receptors.
[b] All assays were conducted using human peripheral blood mononuclear cells (hPBMCs) isolated from human whole blood. Interferon gamma (INFγ) biosynthesis and CellTiter-Glo® (CTG) cellular ATP measurement were used as controls to monitor for off-target cytokine activity and aberrant cytotoxicity, respectively. n.d. = not determined.

cellular potency, now gave a significantly improved selectivity window over the NRs.

Finally, these potent and selective RORc inverse agonists were progressed into a cytokine biosynthesis assay that monitored their ability to inhibit IL-17A production in anti-CD3/CD28-stimulated human peripheral blood mononuclear cells (PBMCs).[29] Interferon gamma (INFγ) biosynthesis and CellTiter-Glo® (CTG) cellular ATP measurement were also assessed to monitor for off-target cytokine activity and aberrant cytotoxicity, respectively. Compound **44** displayed modest inhibition of IL-17 production in the human PBMC assay ($EC_{50}$ = 0.76 μM) whilst **33**, **41** and **47** were slightly more potent ($EC_{50}$ = 0.27, 0.42 and 0.33 μM, respectively) (Table 4). A particular highlight was the identification of **34** as the most potent inhibitor of IL-17 biosynthesis ($EC_{50}$ = 44 nM) which also did not show inhibition of INFγ or CTG assays, demonstrating that this compound was not broadly inhibiting cytokine production and was not overtly cytotoxic. A six-fold improvement in potency was seen for **34** in the human PBMC assay when compared to homologue **33**. This observation contrasts with their equivalent potencies in the HEK293 cell based assay but was not un-expected since different end points are measured in this primary cell based assay compared to the native human PBMCs.[29] The reversed sulfonamide **34** had excellent selectivity for RORc over RORa and RORb (>1000-fold) and the NRs in our cell assays panel (>1000-fold), together with high potency in the IL-17 biosynthesis assay, which represented a useful profile for further progression. When incubated in human and rat liver microsomes, **34** displayed moderate hepatic clearance ($Cl_{hep}$) values in both species (14 and 21 mL/min/kg, respectively) and the compound was progressed to rat pharmacokinetic studies.[38] Disappointingly, **34** displayed clearance at greater than rat liver blood flow in vivo and thus the utility of this reversed sulfonamide was limited to in vitro studies.

Small molecule RORc inverse agonists, with profiles suitable for progression to in vitro and in vivo screens, continue to be of considerable interest to help delineate the complex role of RORc in normal biology and autoimmune disease. We have described the SAR of a new series which incorporated a reversed tertiary sulfonamide linker. Potent RORc inverse agonists with high cellular potencies and excellent selectivity over ROR isoforms and other NRs have been identified. The hydrophobic nature of the RORc binding pocket has made it challenging to incorporate polar functionality and reduce lipophilicity of the reversed sulfonamide series. Identifying strategies which successfully lower lipophilicity may provide compounds with reduced hepatic clearance and improved solubility which could be progressed to in vivo studies. A co-crystal structure of **48** with the RORc-LBD supported previous observations that silent ligands, agonists, and partial inverse agonists do not disrupt a key H479-Y502 H-bond which results in the RORc protein maintaining an agonist conformation. This contrasts with reported inverse agonist ligands, including **7**, that successfully disrupt this key H-bond. Reversed sulfonamides, including **34**, continue to serve as useful in vitro tools whilst our efforts to identify series which can be progressed to in vivo studies continue. The information from our SAR and co-crystal structure with the RORc-LBD has been applied to other related scaffolds and results from these efforts will be disclosed in future publications.

## Acknowledgments

We thank Russell Scammell, Neil Bayliss and Michael Podmore for analytical LCMS and NMR data and Steve McLachlan, Sarah G. Hymowitz and Robert Hall for their important contributions to the project team. We also thank the Genentech Structural Biology Expression group for cloning and expression experiments and staff at beamline 5.0.2 for their assistance with data collection setup. The Berkeley Center for Structural Biology is supported in part by the National Institutes of Health, National Institute of General Medical Sciences, and the Howard Hughes Medical Institute. The Advanced Light Source is supported by the Director, Office of Science, Office of Basic Energy Sciences, of the U.S. Department of Energy under Contract No. DE-AC02-05CH11231.

## Supplementary data

Supplementary data associated with this article can be found, in the online version, at http://dx.doi.org/10.1016/j.bmcl.2014.10.037.

## References and notes

1. Shi, Y. *Drug Discovery Today* **2007**, *12*, 440.
2. Wurtz, J. M.; Bourguet, W.; Renaud, J. P.; Vivat, V.; Chambon, P.; Moras, D.; Gronemeyer, H. *Nat. Struct. Biol.* **1996**, *3*, 87.
3. Isono, F.; Fujita-Sato, S.; Ito, S. *Drug Discovery Today* **2014**, *19*, 1205.
4. Solt, L. A.; Burris, T. P. *Trends Endocrinol. Metab.* **2012**, *23*, 619.
5. Jetten, A. M.; Joo, J. H. *Adv. Dev. Biol.* **2006**, *16*, 313.
6. Ouyang, W.; Kolls, J. K.; Zheng, Y. *Immunity* **2008**, *28*, 454.
7. Ivanov, I. I.; McKenzie, B. S.; Zhou, L.; Tadokoro, C. E.; Lepelley, A.; Lafaille, J. J.; Cua, D. J.; Littman, D. R. *Cell* **2006**, *126*, 1121.
8. Wang, Y.; Kumar, N.; Solt, L. A.; Richardson, T. I.; Helvering, L. M.; Crumbley, C.; Garcia-Ordonez, R. D.; Stayrook, K. R.; Zhang, X.; Novick, S.; Chalmers, M. J.; Griffin, P. R.; Burris, T. P. *J. Biol. Chem.* **2010**, *285*, 5013.
9. Jin, L.; Martynowski, D.; Zheng, S.; Wada, T.; Xie, W.; Li, Y. *Mol. Endocrinol.* **2010**, *24*, 923.
10. Ingraham, H. A.; Redinbo, M. R. *Curr. Opin. Struct. Biol.* **2005**, *15*, 708.
11. Fujita-Sato, S.; Ito, S.; Isobe, T.; Ohyama, T.; Wakabayashi, K.; Morishita, K.; Ando, O.; Isono, F. *J. Biol. Chem.* **2011**, *286*, 31409.
12. Huh, J. R.; Leung, M. W.; Huang, P.; Ryan, D. A.; Krout, M. R.; Malapaka, R. R.; Chow, J.; Manel, N.; Ciofani, M.; Kim, S. V.; Cuesta, A.; Santori, F.; Lafaille, J.; Xu, H.; Gin, D.; Rastinejad, F.; Littman, D. *Nature* **2011**, *472*, 486.

13. Xu, T.; Wang, X.; Zhong, B.; Nurieva, R.; Ding, S.; Dong, C. *J. Biol. Chem.* **2011**, *286*, 22707.
14. Hirose, T.; Smith, R. J.; Jetten, A. M. *Biochem. Biophys. Res. Commun.* **1976**, *1994*, 205.
15. Marciano, D. P.; Chang, M. R.; Corzo, C. A.; Goswani, D.; Lam, V. Q.; Pascal, B. D.; Griffin, P. R. *Cell Metab.* **2014**, *19*, 193.
16. Wang, Y.; Cai, W.; Zhang, G.; Yang, T.; Liu, Q.; Cheng, Y.; Zhou, L.; Ma, Y.; Cheng, Z.; Lu, S.; Zhao, Y.-G.; Zhang, W.; Xiang, Z.; Wang, S.; Yang, L.; Wu, Q.; Orband-Miller, L. A.; Xu, Y.; Zhang, J.; Gao, R.; Huxdorf, M.; Xiang, J.-N.; Zhong, Z.; Elliott, J. D.; Leung, S.; Lin, X. *Bioorg. Med. Chem.* **2014**, *22*, 692.
17. Solt, L. A.; Kumar, N.; Nuhant, P.; Wang, Y.; Lauer, J. L.; Liu, J.; Istrate, M. A.; Kamenecka, T. M.; Roush, W. R.; Vidović, D.; Schürer, S. C.; Xu, J.; Wagoner, G.; Drew, P. D.; Griffin, P. R.; Burris, T. P. *Nature* **2011**, *472*, 491.
18. Skepner, J.; Ramesh, R.; Trocha, M.; Schmidt, D.; Baloglu, E.; Lobera, M.; Carlson, T.; Hill, J.; Orband-Miller, L. A.; Barnes, A.; Boudjelal, M.; Sundrud, M.; Ghosh, S.; Yang, J. *J. Immunol.* **2014**, *192*, 2564.
19. Pantelyushin, S.; Haak, S.; Ingold, B.; Kulig, P.; Heppner, F. L.; Navarini, A. A.; Becher, B. *J. Clin. Invest.* **2012**, *122*, 2252.
20. Chang, M. R.; Lyda, B.; Kamenecka, T. M.; Griffin, P. R. *Arthritis Rheum.* **2014**, *66*, 579.
21. Patel, D. D.; Lee, D. M.; Kolbinger, F.; Antoni, C. *Ann. Rheum. Dis.* **2013**, *72*, 116.
22. http://www.jt.com/investors/results/S_information/pharmaceuticals/pdf/P.L.20140424_E.pdf (article accessed 23 June 2014).
23. Houck, K. A.; Borchert, K. M.; Hepler, C. D.; Thomas, J. S.; Bramlett, K. S.; Michael, L. F.; Burris, T. P. *Mol. Gen. Metab.* **2004**, *83*, 184.
24. Kojetin, D. J.; Burris, T. P. *Nat. Rev. Drug Disc.* **2014**, *13*, 197.
25. Fauber, B. P.; Magnuson, S. *J. Med. Chem.* **2014**, *57*, 5871.
26. Fauber, B. P.; René, O.; Burton, B.; Everett, C.; Gobbi, A.; Hawkins, J.; Johnson, A. R.; Liimatta, M.; Lockey, P.; Norman, M.; Wong, H. *Bioorg. Med. Chem. Lett.* **2014**, *24*, 2182.
27. Fauber, B. P.; René, O.; Boenig, G.; Burton, B.; Deng, Y.; Eidenschenk, C.; Everett, C.; Gobbi, A.; Hymowitz, S. G.; Johnson, A. R.; La, H.; Liimatta, M.; Lockey, P.; Norman, M.; Ouyang, W.; Wang, W.; Wong, H. *Bioorg. Med. Chem. Lett.* **2014**, *24*, 3891.
28. See the Supplementary data for representative synthetic schemes. For representative protocols and characterisation of the analogues, see (a) van Niel, M. B.; Fauber, B. P.; René, O.; Ward, S. WO 2014 090710; (b) van Niel, M. B.; Fauber, B. P.; Gaines, S.; Killen, J.; René, O.; Ward, S. WO 2014 090712.
29. Fauber, B. P.; Boenig, G.; Burton, B.; Eidenschenk, C.; Everett, C.; Gobbi, A.; Hymowitz, S. G.; Johnson, A. R.; Liimatta, M.; Lockey, P.; Norman, M.; Ouyang, W.; René, O.; Wong, H. *Bioorg. Med. Chem. Lett.* **2013**, *23*, 6604.
30. Leach, A. R.; Hann, M. M.; Burrows, J. N.; Griffen, E. J. *Mol. Biosyst.* **2006**, *2*, 429.
31. Leeson, P. D.; Springthorpe, B. *Nat. Rev. Drug Disc.* **2007**, *6*, 881.
32. Waring, M. J. *Expert Opin. Drug Discov.* **2010**, *5*, 235.
33. Hann, M. M. *Med. Chem. Commun.* **2011**, *2*, 349.
34. Ritchie, T. J.; Macdonald, S. J. F. *Drug Discovery Today* **2009**, *14*, 1011.
35. Ritchie, T. J.; Macdonald, S. J. F.; Young, R. J.; Pickett, S. D. *Drug Discovery Today* **2011**, *16*, 164.
36. Ishikawa, M.; Hashimoto, Y. *J. Med. Chem.* **2011**, *54*, 1539.
37. See the Supplementary data for the experimental details associated with the co-crystal structure of the RORc-LBD with compound **48**. The coordinates and structure factors for the complex between RORc and compound **48** have been deposited with the Protein Data Bank and assigned the accession code 4WLB. A binding site interaction map of **7** and **48** with RORc is also shown.
38. See the Supplementary data for the experimental details of the pharmacokinetic study.